JOURNAL OF SPACECRAFT AND ROCKETS
Vol. 44, No. 3, May–June 2007

Weight Growth Study of Reusable Launch Vehicle Systems

Adam F. Dissel* and Ajay P. Kothari†
Astrox Corporation, College Park, Maryland 20740
John W. Livingston‡
Aerospace Systems Design and Analysis ASC/XRE, Wright–Patterson Air Force Base, Ohio 20742
and
Mark J. Lewis§
University of Maryland, College Park, Maryland 20742

DOI: 10.2514/1.26064

Using a wide spectrum of completed air-breathing and rocket-powered launch vehicle baseline configurations, an assessment was undertaken to ascertain each vehicle system's scaling response to empty weight growth. To establish the growth behavior, each vehicle's baseline solution was modified for percentage increases or decreases in the baseline empty weight from $+10\%$ to -10%, after which each vehicle system was then re-solved. The identification of the trends in these solutions enabled the determination of the growth factor for each vehicle configuration. The growth factor characterizes the system's sensitivity to changes in structural weight arising from technological uncertainty. Systems with high growth factors represent a greater amount of design risk because they may rapidly scale out of control if expected technology levels fail to materialize. This understanding may also be applied to measure the extent of improvements possible from application of more advanced technology. Several other figures of merit were also used to evaluate the growth solutions, including empty weight, wetted area, and gross weight. The assessment concluded that single-stage air breathers have a higher response to weight uncertainty than two-stage configurations with the horizontal takeoff mode being more sensitive than vertical takeoff. Two-stage air-breathing configurations, whereas exhibiting lower growth factors, differed greatly from each other in total empty weight across the growth cases with the vertical takeoff mode roughly half the weight of comparable horizontal takeoff configurations. Two-stage reusable rocket configurations also show low scaling weight growth factors and empty weights and are relatively insensitive to small percentage growth changes.

Nomenclature

f_{FX}	=	fixed weight fraction
f_P	=	propellant fraction
f_S	=	baseline scaling structural fraction
f_{SN}	=	scaling structural fraction
GF_{FW}	=	fixed weight growth factor
GF_{SW}	=	scaling weight growth factor
W_E	=	empty weight
W_{FX}	=	fixed weight
W_G	=	gross weight
W_P	=	propellant weight
W_{PAY}	=	payload weight
W_S	=	scaling weight
W_{SN}	=	new scaling weight

I. Introduction

DURING the past two decades, there have been several failed attempts at the development of reusable rocket or air-breathing launch vehicle systems. Single-stage-to-orbit (SSTO) vehicle concepts such as the National Aerospace Plane (NASP), the Mcdonnell Douglas Delta Clipper Experimental (DCX), and the Lockheed Martin X-33 are among those programs canceled. A contributing cause to the demise of these programs was the impact of vehicle growth arising from inaccurate predictions in the attainable level of technology. This phenomenon was particularly apparent in the NASP program, which, by the time of its cancellation, had grown in physical scale many times beyond initial forecasts. The X-33 met a similar fate when the expected propellant tank weight became unachievable due to technology problems with the planned composite tanks. The substitution of heavier, more traditional tanks into the nearly complete vehicle would have resulted in a system now unable to meet its mission goals.

The incorporation of a healthy design margin is a widespread approach to addressing such growth problems in launch vehicles and has been used routinely in aircraft design and sizing. However, launch vehicles possess a much steeper growth response than most aircraft, and whereas a significant design margin may mitigate the growth risk of a multistage launch vehicle, even a 50% margin can be insufficient for a single-stage launcher. A successful reusable launch vehicle program must understand and compensate for these growth effects and focus its efforts on both the realistic estimation of used technology levels and the targeted improvement of those technologies with the greatest system growth impact. This consideration is doubly important for immature and evolving technologies such as hypersonic air-breathing propulsion.

The work presented in this paper represents a broad effort to characterize the growth behavior of a wide-ranging suite of potential reusable launch vehicles for access to space. The reference mission for each configuration solution is a 20,000 lb payload placed into a 100 nm low Earth orbit (LEO). The configurations considered extend across the spectrum of both SSTO and two-stage-to-orbit (TSTO) air-breathing and rocket vehicles and hybrid combinations of the two and includes both horizontal-takeoff-horizontal-landing (HTHL) and vertical-takeoff-horizontal-landing (VTHL) flight modes. The goal of this growth study is *not* to present a single best vehicle design or launch mode; rather, the investigation seeks to characterize the

Presented as Paper 4369 at the 41st AIAA/ASME/SAE/ASEE Joint Propulsion Conference & Exhibit, Tucson, AZ, 10–13 July 2005; received 7 August 2006; revision received 2 November 2006; accepted for publication 28 November 2006.

*Research Engineer, also Graduate Research Assistant, University of Maryland; adissel@umd.edu. Student Member AIAA.
†President, 3500 Marlbrough Way Suite 100. Senior Member AIAA.
‡System Design Engineer, Aeronautical Systems Center/Aerospace Systems Design and Analysis.
§Professor, Department of Aerospace Engineering. Fellow AIAA.

growth sensitivity and resulting design risk that must be addressed to be successful with each given configuration.

II. Design Methodology

All vehicles in this design study have been configured with the HySIDE code developed by Astrox Corp. [1]. The code is a component-based, object-oriented design package within a systems engineering software environment. HySIDE uses analytical solutions and tabulated data as available rather than detailed computational fluid dynamic solutions to be speedy and flexible while still maintaining a high degree of accuracy. Use of the code's rapid design and analysis capabilities allows for the quick systematic comparison of hundreds of design parameters and input cases.

To design a hypersonic vehicle, the code uses the freestream Mach number and altitude at a chosen design point and specified bow shock strength, from which the method of characteristics and streamline tracing methods [2] are used to form the inlet surface. After the trace, the surface inviscid forces are known, as is the inlet exit flow state. A quasi-one-dimensional combustor model is used to model the mixing and burning of hydrogen or hydrocarbon, and a combustor surface is defined. The nozzle flowfield is then also created using the method of characteristics. An external surface joins the inlet capture area and nozzle exit. A reference temperature boundary layer method is then applied to determine the viscous forces, heat transfer, and boundary layer displacement thickness on each surface. The aerodynamic forces are determined by integrating the pressures on each surface's gridpoints [3]. A rocket vehicle is analyzed with similar methods, but without the internal flowpath surfaces.

The code has the ability to perform analysis in a completely integrated fashion (propulsion–airframe–massproperties–aero–gravloss–heating–volumes, etc.). Individual components include either hypersonic air-breathing or rocket engines integrated into a full vehicle model; their performance is calculated over the complete mission trajectory. Vehicle sizing is done in an iterative loop. The vehicle is scaled until the volume available for the fuel is equal to the fuel volume needed based on individual component weights and densities. The code calculates the volumes and areas of all the components and from this subtracts the volumes of payload, equipment, thermal protection system (TPS), etc. The resulting volume is multiplied by a tank packaging efficiency as a measure of how well the tank shape is able to use the available volume. The resulting value is the volume available for propellant, and must equal the fuel volume required to complete the mission trajectory to "close" the vehicle. All of the components will require resizing as the vehicle is continuously scaled to match all of these requirements simultaneously.

Several standard codes, such as Missile Datcom for aerodynamics, have been integrated into the code's suite of analysis tools. Setup time for the complete analysis of a new system requires several days, and once the included components of the specific vehicle system are connected, the system calculations for each solution run are done in about ten minutes on a standard desktop PC. The code has the ability to model 21 different commercially available rocket engines as well as air-breathing scramjet-based engines and traditional turbine engines using a variety of inlet geometries. Reusable and expendable rocket geometries are also included.

III. Alternative Configurations

The baseline versions of the 18 configurations analyzed for this study were set up and solved during previous investigations as documented in [4,5]. Figure 1 identifies these configurations and their baseline gross takeoff weights (GTOW) [the Space Transportation System (STS) and XB-70 Valkyrie are included for scale reference]. As seen from the figure, the study investigated 18 vehicle configurations: nine SSTO and nine TSTO. All of the SSTO vehicles were hypersonic air-breathing vehicles differing by inlet type, propellant selection, low-speed propulsion cycle, and takeoff mode. The TSTO configurations included three pure-rocket systems as well as air-breathing vehicles combined with either an upper-stage rocket orbiter or first-stage rocket booster. The air-breathing vehicles used either an inward-turning "IN" inlet or more traditional wedge "2D"-type inlet geometry. The low-speed propulsion cycles for all

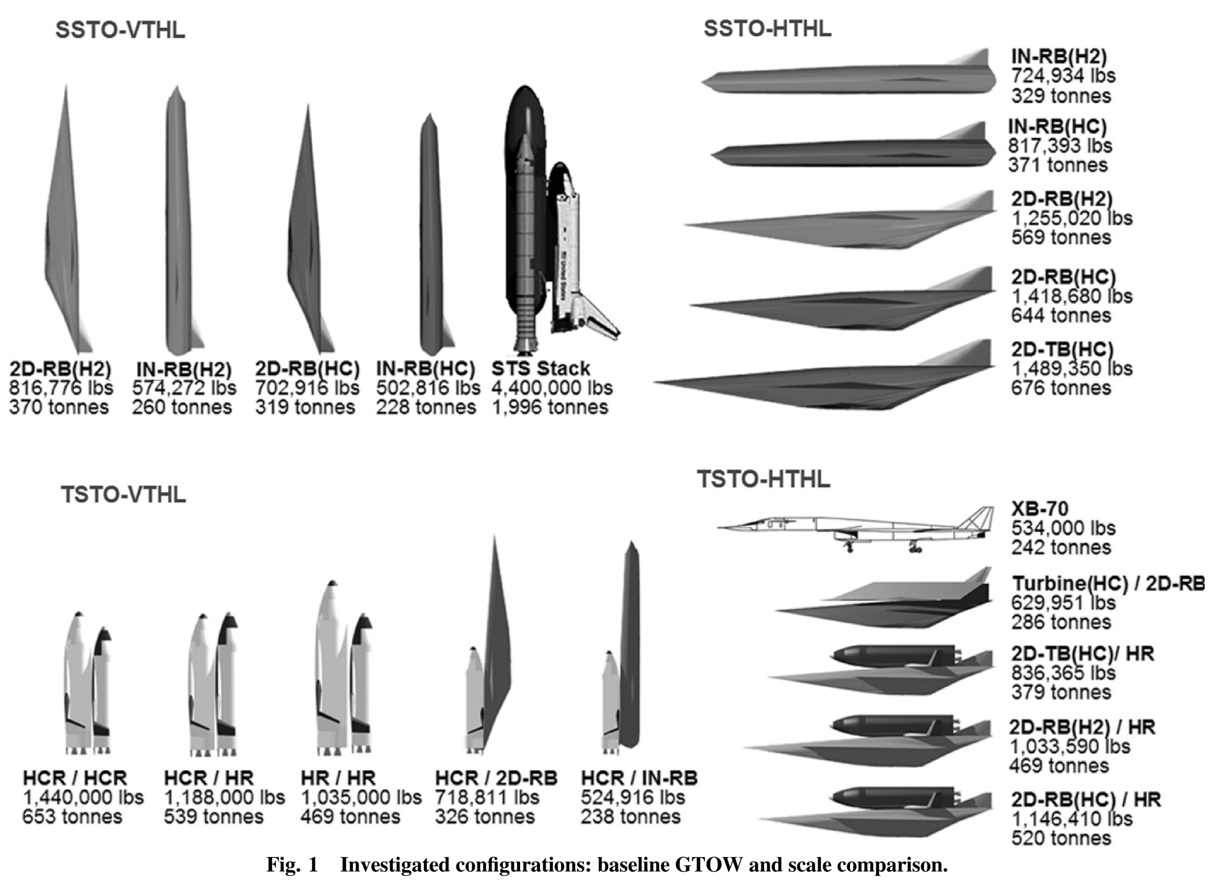

Fig. 1 Investigated configurations: baseline GTOW and scale comparison.

Table 1 Investigated configurations: propellant and empty weight fractions

Vehicle name	Configuration type	Propellant fraction					Empty weight fraction				
		−10%	−5%	0%	+5%	+10%	−10%	−5%	0%	+5%	+10%
IN-RB(H2)	SSTO VTHL	0.729	0.729	0.729	0.730	0.730	0.224	0.230	0.236	0.241	0.246
IN-RB(HC)	SSTO VTHL	0.754	0.754	0.754	0.754	0.755	0.195	0.201	0.206	0.211	0.216
2D-RB(H2)	SSTO VTHL	0.755	0.754	0.752	0.752	0.752	0.213	0.218	0.223	0.228	0.232
2D-RB(HC)	SSTO VTHL	0.777	0.777	0.776	0.776	0.776	0.185	0.190	0.195	0.200	0.203
IN-RB(H2)	SSTO HTHL	0.727	0.728	0.728	0.728	0.730	0.231	0.238	0.245	0.250	0.255
IN-RB(HC)	SSTO HTHL	0.757	0.757	0.757	0.758	0.762	0.207	0.214	0.219	0.224	0.229
2D-RB(H2)	SSTO HTHL	0.754	0.753	0.752	0.752	0.753	0.220	0.227	0.232	0.237	0.241
2D-RB(HC)	SSTO HTHL	0.780	0.780	0.778	0.779	no soln	0.197	0.203	0.207	0.212	no soln
2D-TB(HC)	SSTO HTHL	0.700	0.700	0.701	no soln	no soln	0.279	0.282	0.286	no soln	no soln
HR/HR	TSTO VTHL	0.795	0.792	0.790	0.787	0.785	0.182	0.187	0.191	0.195	0.199
HCR/HR	TSTO VTHL	0.847	0.845	0.843	0.842	0.840	0.133	0.136	0.139	0.141	0.145
HCR/HCR	TSTO VTHL	0.873	0.871	0.869	0.868	0.866	0.111	0.113	0.116	0.119	0.121
HCR/IN-RB	TSTO VTHL	0.756	0.754	0.752	0.751	0.750	0.198	0.205	0.210	0.215	0.219
HCR/2D-RB	TSTO VTHL	0.772	0.770	0.768	0.767	0.765	0.194	0.199	0.204	0.208	0.213
2D-RB(H2)/HR	TSTO HTHL	0.719	0.713	0.706	0.700	0.694	0.257	0.265	0.275	0.283	0.290
2D-RB(HC)/HR	TSTO HTHL	0.746	0.740	0.735	0.727	0.722	0.233	0.241	0.248	0.257	0.264
2D-TB(HC)/HR	TSTO HTHL	0.613	0.602	0.593	0.585	0.576	0.358	0.371	0.383	0.394	0.404
Tutbine/2D-RB	TSTO HTHL	0.512	0.500	0.489	0.481	0.473	0.448	0.464	0.479	0.491	0.502

air breathers was provided by either integrated rockets "-RB" or turbines "-TB" operating on hydrogen "(H2)" or hydrocarbon "(HC)" fuel. All air breathers assumed hydrogen scramjets and integrated hydrogen rockets for postscramjet ascent to orbit. One HTHL vehicle used a pure turbine-powered booster as a first stage. Where used, the pure-rocket stages are notated by propellant; hydrocarbon-fueled rockets (HCR) or hydrogen-fueled rockets (HR). The TSTO notation in the figures is listed as "Stage1/Stage2."

In addition to the baseline solutions, this study used the design code to produce four additional growth solutions for each system concept, which corresponded to percentage changes in the total baseline empty weight for −10, −5, +5, and +10%. These data solutions are required to determine the sensitivity or growth factor for each of the concepts. The propellant and empty weight fractions for the closed data points for the different empty weight growth percentages are shown in Table 1.

The tabulated data show that, with the exception of the largest TSTO air breathers, the majority of the configurations exhibit very small changes in propellant fraction across the different growth solutions. This observation supports the simplification that the propellant fraction can be considered approximately constant.

A. Sizing Equations and Growth Factors

Insight into how vehicle systems are sized can be had by developing and examining a set of relatively simple equations derived from the "sizing equation." These expressions can be employed to determine the weight impact of different growth scenarios without the need to re-solve each system in detail. For the purposes of this analysis, the total vehicle weight is divided into four categories: propellant weight, fixed weight, scaling weight, and payload weight. The propellant weight includes all propellants used for launch ascent, as well as for orbital positioning and maneuvering. The fixed weight is the sum of all the vehicle components that do *not* scale with vehicle sizing during closure, such as payload bay fixtures and mounts, payload bay doors, nonscaling avionics, etc. The scaling weight is the sum of the weights of the spacecraft that *do* scale with increasing or decreasing size. Most major subsystems and structure items fall into this category, including propellant tanks, thermal protection surfaces, airframe, wings, landing gear, engines, etc. The vehicle gross weight is the sum of all four weight categories:

$$W_G = W_P + W_{FX} + W_S + W_{PAY} \tag{1}$$

The scaling and propellant weight fractions are simply the respective weights divided by the total gross weight:

$$f_S = \frac{W_S}{W_G} \tag{2}$$

$$f_P = \frac{W_P}{W_G} \tag{3}$$

To determine the growth factors, a sizing equation is needed that properly captures the scaling behavior seen in the design code solutions. It will be useful to express the gross weight in terms of the fixed weight, and scaling and propellant weight fractions:

$$W_G = \frac{W_{PAY} + W_{FX}}{1 - f_S - f_P} \tag{4}$$

This sizing equation is very useful for a wide range of aircraft types and missions. The scaling and propellant weight fractions are indeed quite close to constant over a reasonably large range of sizes for a given design layout, engine design, and mission. The empty weight is simply the sum of both the scaling and fixed structural weights:

$$W_E = W_S + W_{FX} = f_S W_G + W_{FX} \tag{5}$$

Substituting for gross weight, an empty weight equation is obtained in terms of the scaling weight fraction and fixed weight:

$$W_E = f_S \frac{W_{PAY} + W_{FX}}{1 - f_S - f_P} + W_{FX} \tag{6}$$

Equations (4) and (6) yield the gross and empty weights as functions of fixed weight, payload weight, propellant fraction, and scaling structure fraction. For constant values of fixed weight and payload weight, the vehicle may be sized with the two fractions.

B. Correction with Analysis Results

The preceding sizing equations will require values for the scaling weight fraction and the vehicle fixed weight that will enable the equations to approximate the gross and empty weights of the data solutions. To this point, there has been no effort made to distinguish the empty weight into either scaling or fixed weight types. Presupposed values for these quantities that could have been part of the design setup will likely not produce sufficient data agreement if used in the sizing equations. The discrepancy is attributable to the nonlinear behavior of the solution of an integrated vehicle. Component level weight estimations are based on many varied parameters; some items scale with surface area or vehicle volume, whereas others are determined based on the gross or empty weights. The fixed weight and scaling weight fractions are varied until they best fit the actual design code data points, in effect determining how much of the empty weight is actually behaving as fixed weight vs scaling weight. Negative values of the term reduce the amount of empty weight acting like fixed weight, whereas positive values increase the amount. Figures 2 and 3 illustrate the effect of different

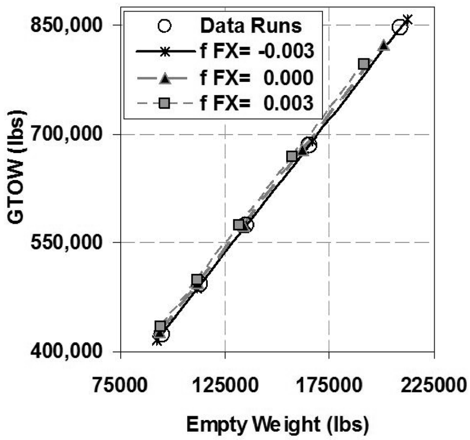

Fig. 2 GTOW matching with IN-RB(H2) data.

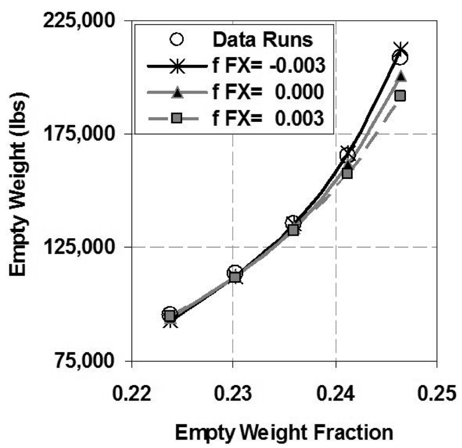

Fig. 3 EW matching with IN-RB(H2) data.

values of f_{FX} in matching the gross and empty weights of the design code data points.

The figures show that for the VTHL SSTO IN-RB(H2) vehicle, a good data agreement is achieved with a f_{FX} value of -0.003. The scaling fraction is then simply the empty fraction minus the fixed weight fraction. The fixed and scaling weight fractions were accordingly determined for each of the configurations. We now have smooth analytic relationships for each of our alternative designs, which can be differentiated to determine growth behavior.

IV. Empty Weight Growth Factors

An empty weight growth factor is a measure of the scaling response in vehicle empty weight due to an increase in either the vehicle's fixed weight or scaling weight. The fixed weight growth factor determines the change in a given vehicle system's empty weight for an increase in the fixed weight of the system, as would occur for an increased payload requirement; whereas the scaling weight growth factor reflects the change in empty weight due to a change in the vehicle's own scaling structural weight.

A. Fixed Weight Growth Factor

An increased fixed weight requirement will trigger an increase in the vehicle's size as it is scaled up to closure. The growth response is straightforward, because the vehicle model weight estimating parameters do not change for changes in fixed weight, remaining fixed at the baseline values. The fixed weight growth factor is the derivative of the empty weight in Eq. (6) taken with respect to the fixed weight and will be a constant value for a given system and suite of technology assumptions.

$$\frac{dW_E}{dW_{FX}} = \frac{f_S}{1 - f_S - f_P} + 1 \tag{7}$$

The fixed weight growth factor may be expressed in terms of weight or the weight fraction:

$$GF_{FW} = \frac{W_{PAY} + W_{FX} + W_S}{W_{PAY} + W_{FX}} \tag{8}$$

$$GF_{FW} = \frac{1 - f_P}{1 - f_S - f_P} \tag{9}$$

B. Scaling Weight Growth Factor

The scaling weight growth factor is a measure of the scaling response in vehicle empty weight to an increase in the unit weight of the vehicle structure. This increase often arises due to a change in the estimation of the corresponding weight of some structural technology, such as a heavier or lighter weight TPS tile type. The scaling weight growth factor can therefore be used as a measure of the vehicle's response to the technological uncertainty inherent in the development of any future system, and as such was the principal figure of merit applied in this investigation. A general aerospace vehicle scaling reaction to such an increase proceeds as follows:

1) A previously closed vehicle solution experiences an increase in a structural unit weight.

2) That percentage increase multiplied by the total amount of that structural component present in the closed solution results in an additional amount of weight that must now be carried by the vehicle.

3) The vehicle solution is no longer closed, meaning it no longer contains sufficient fuel to successfully execute the mission with the now heavier vehicle. The weight addition acts as a perturbing influence that triggers a scaling up of the vehicle solution to reclose the vehicle.

4) As the vehicle grows in response to the weight change it must also now do so with a correspondingly higher unit weight. This double impact causes a much larger change in the reclosed vehicle's empty weight vs the original empty weight than just the addition of the perturbing change in structure weight alone.

5) The empty weight growth factor is obtained by differentiating the empty weight scaling Eq. (6) with respect to the weight change and is the slope of the delta empty weight/delta perturbing weight curve at the point of the vehicle solution.

As previously mentioned, each vehicle system was reclosed in HySIDE for percentage increases in the total baseline structural (empty) weight from -10% to $+10\%$. The empty and gross weight sizing equations were applied to curve fit through the five solution points for each system. For reasons that will become clear further on, the empty weight equation is first rewritten in terms of a new scalable weight W_{SN}:

$$W_E = \left(\frac{W_{SN}}{W_G}\right) \frac{W_{PAY} + W_{FX}}{1 - W_{SN}/W_G - f_P} + W_{FX} \tag{10}$$

Differentiating with respect to the scalable weight yields

$$\frac{dW_E}{dW_{SN}} = \left(\frac{1}{W_G}\right) \frac{W_{PAY} + W_{FX}}{1 - W_{SN}/W_G - f_P} + \left(\frac{W_{SN}}{W_G}\right) \frac{W_{PAY} + W_{FX}}{(1 - W_{SN}/W_G - f_P)^2 W_G} \tag{11}$$

Pulling the common terms to the front of the equation,

$$\frac{dW_E}{dW_{SN}} = \left(\frac{1}{W_G}\right) \frac{W_{PAY} + W_{FX}}{1 - W_{SN}/W_G - f_P} \left[1 + W_{SN} \frac{1}{(1 - W_{SN}/W_G - f_P) W_G}\right] \tag{12}$$

Simplifying the bracketed term in the preceding equation gives

$$\frac{\mathrm{d}W_E}{\mathrm{d}W_{\mathrm{SN}}} = \left(\frac{1}{W_G}\right)\frac{W_{\mathrm{PAY}} + W_{\mathrm{FX}}}{1 - f_{\mathrm{SN}} - f_P}\left(\frac{1 - f_P}{1 - f_S - f_P}\right) \tag{13}$$

The final step is to substitute equivalent fractions for the weights. This step reintroduces the original baseline scalable weight fraction f_S and is the reason for the introduction of the new (nonbaseline) scaling weight fraction f_{SN}. It is important to note that at the baseline solution point, $f_{\mathrm{SN}} = f_S$. The scaling weight growth factor is now given by the following equation:

$$\mathrm{GF}_{\mathrm{SW}} = \frac{(1 - f_S - f_P)(1 - f_P)}{(1 - f_{\mathrm{SN}} - f_P)^2} \tag{14}$$

The growth factor may be alternatively expressed in terms of weights:

$$\mathrm{GF}_{\mathrm{SW}} = \frac{(W_{\mathrm{PAY}} + W_{\mathrm{FX}})(W_{\mathrm{PAY}} + W_{\mathrm{FX}} + W_S)}{(W_{\mathrm{PAY}} + W_{\mathrm{FX}} + W_S - W_{\mathrm{SN}})^2} \tag{15}$$

Combining these growth factor equations with those for empty and gross weight allows for the estimation of vehicle weights and growth response by simply choosing different values of the scaling structure fraction. Note that when $f_{\mathrm{SN}} = f_S$, Eqs. (14) and (15) degenerate into Eqs. (8) and (9).

Once obtained, the scaling weight growth factor may be used for quickly performing multiple individual system component technology assessments without the need to re-solve each system separately. Thus employed, the growth factor is a powerful way to determine which configurations pose less of a design risk. Once a particular vehicle's scaling behavior is understood, it can be coupled with further analyses to determine an appropriate design margin. Livingston [6] has combined the growth factor process with defined uncertainty bands on the vehicle technology to determine the growth point required to achieve an 80% probability of successful closure based on the assumed maturity of the technology.

V. Additional Figures of Merit

A. Empty Weight

At this level of analysis, the total vehicle system empty weight may be reasonably employed as the main cost driver of a launch vehicle system. Most of the launch operation and flight refurbishment costs, as well as the initial development and procurement costs of a launch vehicle scale roughly with empty weight [7]. When comparing the empty weights as a rough measure of the approximate cost and feasibility of designing and constructing the vehicle, it should be remembered that the use of conformal tanks, active TPS, and other new technologies will result in an air-breathing vehicle that "pound for pound" will likely cost more than a pure-rocket vehicle. Although existing rocket technology is more mature than the emerging hypersonic air breathers, the requirement for highly operable and reliable rocket engines for post air-breathing orbital ascent will require more investment [8] in rocket engine capabilities.

B. Wetted Area

The amount of wetted area impacts the vehicle's performance, weight, and operational cost. For the heating conditions present during either the air-breathing trajectory or atmospheric reentry, all the exposed area of a hypersonic vehicle will require some level of TPS. When the heating over a certain area exceeds the limits of current materials technology, then those areas must be actively cooled. The reduction of TPS area yields a double benefit, the first being a reduction in weight, and the second a reduction in the time and cost of TPS refurbishment [9]. Conversely, runaway growth in vehicle size leads to multiplying maintenance cost. TPS maintenance is a major part of the space shuttle's refurbishment costs. State of the art and future advanced passive TPS materials may require less maintenance than previous TPS materials. However, the actively cooled panels on future hypersonic vehicles are a new TPS system that is likely to require a fair amount of inspection and between flight refurbishment. The air-breathing stages need substantial active cooling on leading edges and through the inlet, combustor, and nozzle.

C. Gross Weight

Vehicle gross takeoff weight is often cited as a principal metric of comparison between different vehicle configurations. However, the vehicle gross weight is not as useful a figure of merit as the three listed earlier. The major constituents of the gross weight for the vehicles are the propellants required. Compared with the cost of acquiring and maintaining the vehicle, the cost of purchasing, storing, and handling each flight's propellant is nearly insignificant. Although a higher gross weight vehicle for a given design and mission may represent a lower performing propulsion system, it is the impact of that performance on the vehicle's empty weight and surface area that are of primary interest. However, the gross weight was included in this study because it does give quick insight into the scaling of parameters that have to do with the fueled vehicle, such as propulsion thrust requirement, pad limitations, and in the case of horizontally launched vehicles, the wing and landing gear sizing. It is also used to determine if a particular HTHL vehicle baseline or grown solution has exceeded the runway bearing load limitation, which, for this study, was assumed to be 1.5×10^6 lb.

VI. Results

As mentioned, the 18 vehicle configurations were all re-solved for empty weight percentage changes of −10, −5, +5, and +10%, thus representing an additional 72 closed vehicle solutions in addition to the original 18 baseline closures. The discussed measures of merit were determined for each solution point and are presented in the following section. In each of the remaining figures, each individual vehicle system is shown at the five solution points such that the general trend in each is readily estimated. The data thus presented yield valuable insight into a broad range of possible vehicle growths; both positive and negative. If it is determined that the baseline technology assumptions used for this study are too optimistic, one need only shift up to a higher +% solution point on each vehicle growth curve to reassess the impact of a more conservative performance estimate. The growth factor results presented from this point forward are all scaling weight growth factors.

A. Growth Factor Figure Notation

The next two figures show the scaling weight growth factor vs empty weight trends for SSTO and TSTO configurations. The five solutions for each vehicle are represented as points on the figures with trend lines connecting them. The filled symbols represent the baseline solution; the two open symbols below this point are the −5 and −10% solutions, and the two open symbols above the baseline point are the +5 and +10% solutions. There are a few configurations whose closure points extend off above the scale of the figure axis, in which case only the negative percentage solutions may appear.

Represented in Fig. 4 are the scaling weight growth factors vs empty weights for the SSTO air-breathing configurations. The configurations differ by inlet type and low-speed rocket propulsion segment fuel selection. The figure shows that the VTHL inward-turning air breather with a hydrocarbon-fueled, low-speed propulsion segment has the lowest baseline growth factor and empty weight of the SSTO configurations. The VTHL all-hydrogen versions have slightly higher baseline growth factors. This difference becomes magnified as the solutions are run at the +5 and +10% cases. As seen, the distance between the baseline solution point and the +5% point is greater for the vehicles with higher baseline growth factors than for those with lower baseline growth factors. The higher growth response necessitates further scaling to reclose the vehicle. This behavior is only amplified when considering the distance to a further closure point. For example, at the +10% point, the VTHL inward-turning (HC) vehicle has increased its growth factor by 6 and

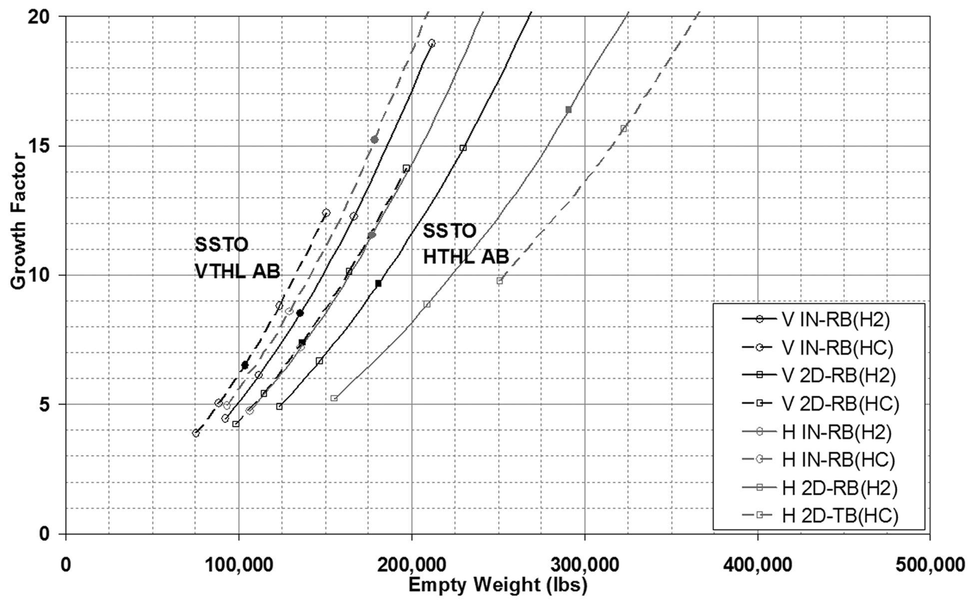

Fig. 4 Growth factor vs empty weight: SSTO, VTHL, and HTHL air breathers.

its empty weight by 50,000 lb, whereas the all-hydrogen version of the same configuration has increased by more than 10 in growth factor and over 80,000 lb in empty weight. Compared to the vertical SSTO vehicles, the baseline solution points for the HTHL configurations are shifted towards higher values of scaling weight growth factor and empty weight. The higher growth factors cause small differences in the configurations to be magnified, thus resulting in a sparser concentration of the baseline solutions than was seen for the VTHL vehicles. This accelerated growth response is due to conditions pertaining to the horizontal takeoff mode of these configurations. The wing area and landing gear of an HTHL vehicle are sized with respect to the vehicle gross weight. As the gross weight increases, these subsystems increase at a faster rate than equivalent systems on VTHL vehicles in which the wing area and landing gear are sized for the smaller empty weight increase. The larger wing area of the HTHL vehicles results in significant drag losses during the high-speed ascent portion of the hypersonic trajectory. These gross weight interactions are also the reason why the use of hydrocarbon fuel in the low-speed rockets used by some of the SSTO HTHL configurations now causes an increase in growth response. The lower performance hydrocarbon fuel drives up the gross weight of the vehicle and thus enters into the wing/gear scaling problem afresh. These factors combined together cause the SSTO HTHL configurations to be more sensitive to growth than the SSTO VTHL configurations. Indeed, for the technological assumptions of the current study, some of the HTHL vehicles are already exhibiting a nearly runaway scaling response at the $+5\%$ closure point. The poorest performer of the four HTHL vehicles shown is the SSTO air breather with integrated turbines for low-speed propulsion. Its baseline point has a very high empty weight and growth factor and does not even appear on the figure, although its lower -5 and -10% closure points do. Having higher growth sensitivity does not summarily invalidate the potential of an SSTO HTHL. For the applied technological estimations, the SSTO VTHL vehicles are an improvement over the SSTO HTHL configurations in terms of empty weights and growth sensitivity. Because the same technology estimates and methods were consistently applied for common subsystems in the solutions of vehicles employing either launch mode, closing the resulting size gap would require large changes to technologies and assumptions peculiar to the particular launch mode. Technological possibilities for improving the performance of the SSTO HTHL vehicles with respect to the SSTO VTHL vehicles

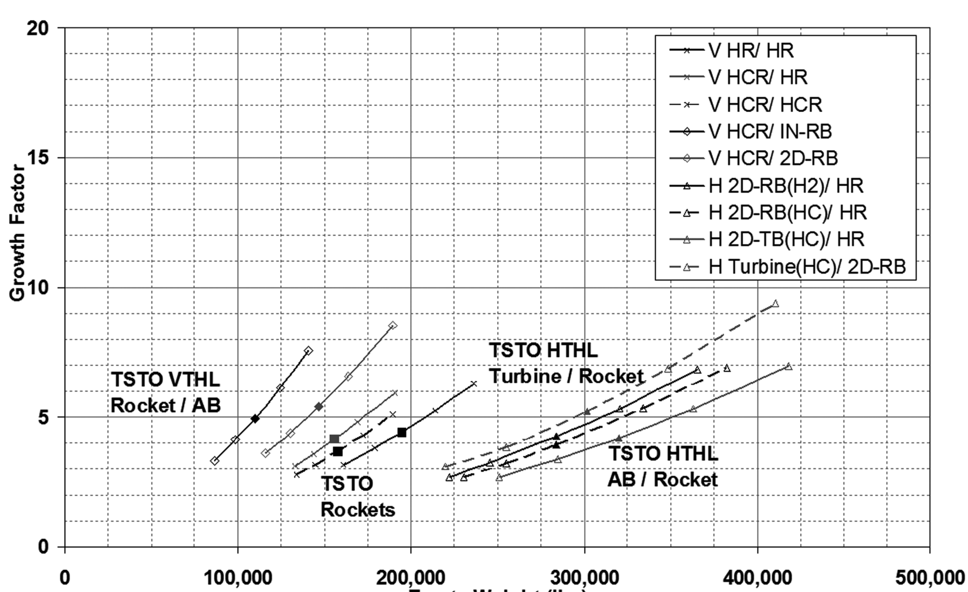

Fig. 5 Growth factor vs empty weight: TSTO configurations.

might include magnetic rail launch or increased takeoff speed. Likewise, the size gap could be reduced by conditions that might adversely and uniquely affect the SSTO VTHL configurations. It is possible that the SSTO VTHL concepts could get larger and the SSTO HTHL concepts could get lighter, but it is unlikely that the gap between them would close completely. The sizing trends observed in these growth trades should be considered carefully; the high degree of growth variability shown in these results for either SSTO launch mode precludes any final selection judgment until the considerable uncertainties in basic hypersonic vehicle component technologies and integration issues are reduced.

The TSTO configurations are considered next, and their growth solutions are shown in Fig. 5. The effect of staging on growth response is quite visibly communicated by the concentrated solutions shown. The empty weight of the three pure-rocket vehicles varies by only ~80, 000 lb across the whole growth percentage range. The smaller changes of the TSTO rockets are indicative of a robust system that is well suited to absorbing moderate changes in weight and therefore exhibits less design risk. Because of the subdued growth behavior of the TSTO rocket configurations, there is little variation among the three vehicles even though their propellant configurations are quite different. Also included in Fig. 5 are two additional TSTO categories that employ either HTHL air-breathing boosters with upper-stage rockets (three vehicles), or an HTHL turbine booster with an upper-stage hypersonic air breather (one vehicle). Once again, the use of staging moderates the scaling response; however, the combined empty weight of the TSTO HTHL systems using air-breathing stages is double that of the TSTO rockets. The TSTO HTHL vehicles show a larger spread in the location of the different closure points, but are still more concentrated than the SSTO HTHL air breathers. Although these configurations only increase a few points in growth factor from the baseline point up to the +10% case, it is important to note that they have gained ~100, 000 lb in empty weight in doing so. The final two configurations of the figure are vertically launched rocket boosters with upper-stage air breathers. These TSTO VTHL vehicles are less than half the empty weight of the previous TSTO HTHL vehicles. These two TSTO VTHL configurations also show fairly low scaling weight growth factors and scaling response; however, they have much steeper trend lines. This may lead to the erroneous conclusion that these vehicles are scaling faster than their TSTO HTHL counterparts. The opposite is actually true; the closure points on the steeper trend indicate less resulting empty weight growth from the same scaling response. The actual +5% solution points for both the VTHL and HTHL configurations are at a growth factor of between 6 and 7, so both categories actually experienced similar growth factor increase but with very different outcomes in terms of empty weight response.

B. Measures of Merit Figure Notation

The next four figures show the results of each closure solution for the general figures of merit chosen for this study. For the following figures, results are only presented for the best two vehicles from each general configuration category with the exception of the SSTO HTHL air-breathing vehicles, where three vehicles were presented to show the results of the SSTO turbine-based vehicle. The results are presented in bar charts with the vehicle closures for the −10% case on the front row, and the +10% case on the back row. Each bar is labeled with the actual solution point data. There are no positive (+%) growth data for the SSTO HTHL turbine-based vehicle on the far right of the figures because that configuration was impossible to close at even the +5% growth case. The +10% solution point for the SSTO HTHL 2D hydrogen rocket-based vehicle is not shown due to blowing up in a similar fashion. A vehicle thumbnail image is included to represent each configuration category and to provide ready identification of each group of data.

Figure 6 represents the scaling weight growth factors across the different closure solutions for the best two vehicles of each configuration category. In the figure, TSTO configurations are to the right, and SSTO configurations are to the left. This figure again

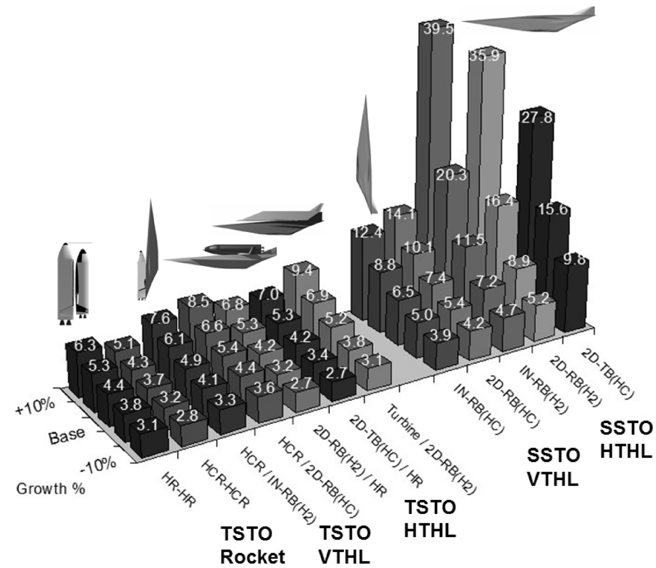

Fig. 6 Empty weight growth factors.

addresses the low growth factors of TSTO configurations vs SSTO. The growth factor data suggest that the development of an immature technology such as hypersonic propulsion should first be applied in a more forgiving TSTO configuration to gain experience and develop the technology and then apply that understanding to the SSTO, in hopes of achieving the lower percentage closure points.

The amounts of total vehicle empty weight for each system are shown in Fig. 7. The empty weight results for the TSTO vehicles differ markedly from each other. The three highest empty weights for the TSTO vehicles are for the two TSTO HTHL configurations and they are double the amount for the two TSTO VTHL configurations. A more detailed analysis of the causes of the differences between these configurations is contained in [5]. The highest empty weights in the SSTO category are also attributed to the SSTO HTHL vehicles, which, due to higher growth response, become larger than the SSTO VTHL vehicles. Another interesting observation is that the three different configurations using turbines for the low-speed trajectory segment have the three highest empty weights of all the configurations studied.

The total wetted area for each vehicle is represented in Fig. 8. The trends seen for wetted area follow the same patterns as those observed for the empty weight. As mentioned, the wetted area is a

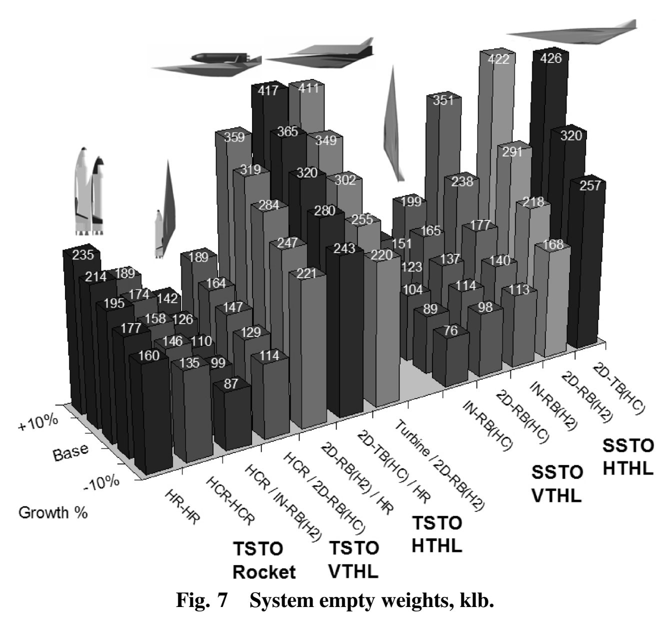

Fig. 7 System empty weights, klb.

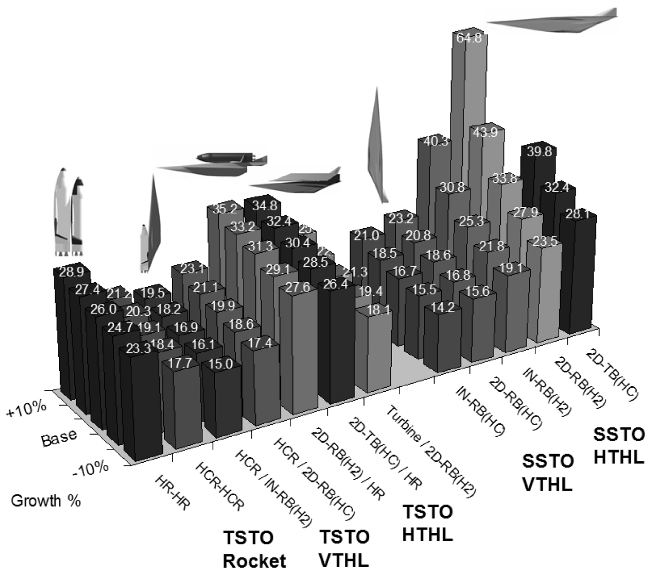

Fig. 8 Total wetted areas, kft^2.

strong driver for the amount of maintenance and refurbishment costs and turn time for a reusable launch vehicle. As with empty weight, not all wetted area is the same. For example, the rockets used as first stage boosters never see any substantial heating and therefore get by with much less capable TPS. In contrast, the hypersonic air-breathing vehicles all require advanced high-temperature passive TPS over every exposed portion of the vehicle's external surface and internal flowpath except for the flowpath regions that are actively cooled.

The final measure of merit is the vehicle gross weight shown in Fig. 9. This is one figure of merit in which the pure rockets come out fairly high due to their higher propellant fractions. The gross weights of some of the SSTO HTHL vehicles in this study have exceeded the assumed runway load limitation of 1.5×10^6 lb for some of the closure solutions. At $+10\%$, all SSTO HTHL air breathers are above this limit with the exception of the all-hydrogen, inward-turning vehicle. The SSTO HTHL turbine-based vehicle is right at the limit already for its baseline case. These solutions were all for 20,000-lb payload to LEO. It is easy to foresee from the trends in this figure that any substantial increase in that payload could invalidate all of the HTHL vehicles at any positive growth percentage from operations staged from existing runways. The SSTO and TSTO VTHL vehicles have the lowest total gross weights of all the vehicles.

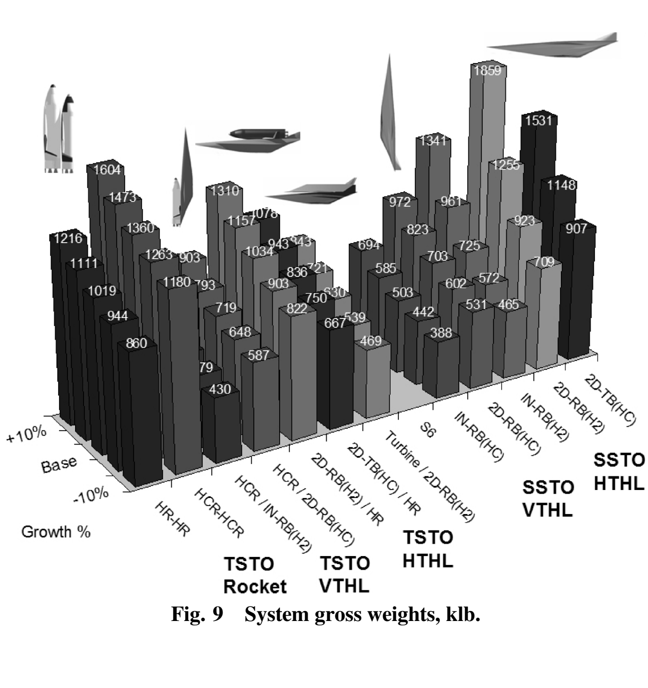

Fig. 9 System gross weights, klb.

VII. Conclusions

This investigation considered 18 vehicle systems, many different configurations of air breathers and rockets, and performed a broad growth investigation to characterize the scaling behavior of each vehicle system. The general growth sensitivity conclusions that may be drawn as a result of this study are listed next. For more detailed conclusions contrasting individual baseline vehicles with each other, the reader is referred to [4,5].

For vertically launched TSTO rockets:

1) The use of staging greatly reduces the scaling behavior of these systems.

2) The three vehicle solutions for this category have very similar scaling weight growth factors and exhibit minor increases in empty weight for even large growth percentages.

3) Design success is very likely through the employment of a moderate growth margin during development.

For SSTO air breathers:

1) SSTO configurations have higher baseline scaling weight growth factors than the TSTO configurations and are highly susceptible to large increases or decreases in weight and scale for even small growth percentages.

2) For the configuration assumptions of the present study, the empty weights and scaling response of the SSTO VTHL configurations was consistently less than that observed for the SSTO HTHL configurations, with the all-hydrogen-fueled SSTO VTHL vehicles being more variable than those with hydrocarbon-fueled, low-speed propulsion segments.

3) For the HTHL SSTO configurations, the use of hydrocarbon rocket propulsion for the low-speed segment and its corresponding increase in vehicle gross weight exacerbates the growth response compared to the all-hydrogen configurations. The SSTO turbine vehicle had the highest baseline empty weight and most severe scaling response of all the configurations studied.

For TSTO air breathers:

1) As with the TSTO rockets, the use of staging benefits the TSTO air-breathing vehicles, both VTHL and HTHL.

2) Although the HTHL TSTO air breathers exhibit low growth factors (compared to SSTO), the magnitudes of the changes in weight and scale for larger growth percentages is considerable due to the higher baseline empty weights of these configurations.

3) The VTHL TSTO air breathers are consistently less than half of the total empty weight of the HTHL TSTO configurations across the applied growth percentages. Although similar to the HTHL TSTO air breathers in growth factor, the magnitudes of the changes in empty weight and scale are much less at the higher growth percentages.

Many of these observed trends have been recently corroborated by other researchers. The configurations investigated by Hank et al. [10] were analogous to many of those presented here. Other SSTO configurations were examined by Orloff , which, although similar to those of this study, used additional propellant configurations such as completely hydrocarbon-fueled configurations and vehicles using duel-fuel scramjets.

In summary, a sufficient understanding and allowance for the growth response of a particular launch configuration is vital in helping to assure a successful vehicle program. As applied to an SSTO configuration, this understanding and determination becomes of paramount importance due to the severity of the scaling response. This makes it nearly impossible to accurately set the final scale and size of the vehicle unless there is near-perfect certainty in the performance and technology of the system beforehand. Failure to appreciate or account for the severity of that response has directly contributed to the demise of previous SSTO attempts. Indeed, there are many areas of basic research ranging from the estimation of conformal hydrogen tank weight to the accounting of trim-drag and aeroelastic effects that must be addressed before the highly growth-sensitive SSTO configurations can be designed with more certainty. The TSTO configurations have lower scaling weight growth factors, indicating vehicle systems that more easily absorb design or technology changes during the development program without extreme increases in size and weight. A program with such a vehicle is many times more likely to be successful at incorporating the actual design numbers once the vehicle design has been frozen. The use of staging is a very beneficial way to reduce growth behavior and provides an intermediate point where uncertain or emerging technologies may be applied and matured in a system with a lower inherent design risk before being attempted on a more exacting SSTO configuration. A high scaling weight growth factor does *not* necessarily invalidate a particular vehicle design; it is just a measure of how much more certainty and confidence must be had in the solution parameters to be successful with that design.

Acknowledgments

Funding for this work was provided by the U.S. Air Force Research Laboratory, Air Vehicles Directorate (AFRL/VA) contract No. F33615-03-C-3319. The authors are grateful for the assistance of V. Raghavan of Astrox. Astrox Corporation would like to express particular thanks to Don Paul, AFRL/VA, Jess Sponable, AFRL/VA, and Dan Tejtel, AFRL/VA of Wright–Patterson AFB, Ohio for their consistent support and insight.

References

[1] Kothari, A. P., Tarpley, C., McLaughlin, T. A., Suresh Babu, B., and Livingston, J. W., "Hypersonic Vehicle Design Using Inward Turning Flowfields," AIAA Paper 96-2552, July 1996.

[2] Billig, F. S., and Kothari, A. P., "Streamline Tracing, a Technique for Designing Hypersonic Vehicles," ISABE Paper 33.1, Sept. 1997.

[3] Kothari, A. P., Tarpley, C., and Pines, D., "Low Speed Stability Analysis of the Dual Fuel Waverider Configuration," AIAA Paper 96-4596, Nov. 1996.

[4] Dissel, A. F., Kothari, A. P., and Lewis, M. J., "Comparison of Horizontally and Vertically Launched Air-Breathing and Rocket Vehicles," *Journal of Spacecraft and Rockets*, Vol. 43, No. 1, 2006, pp. 161–169.

[5] Dissel, A. F., Kothari, A. P., and Lewis, M. J., "Investigation of Two-Stage-to-Orbit Air-Breathing Launch Vehicle Configurations," *Journal of Spacecraft and Rockets*, Vol. 43, No. 3, 2006, pp. 568–574.

[6] Livingston, J. W., "Comparative Analysis of Rocket and Air-breathing Launch Vehicles," AIAA Paper 2004-6111, Sept. 2004

[7] Bowcutt, K., Gonda, M., Hollowell, S., and Ralston, T., "Performance, Operational and Economic Drivers of Reusable Launch Vehicles," AIAA Paper 2002-3901, July 2002.

[8] Bowcutt, K., and Hatakeyama, S. J., "Challenges, Enabling Technologies and Technology Maturity for Responsive Space," AIAA Paper 2004-6005, 2004.

[9] Rooney, B. D., and Hartong, A., "A Discrete-Event Simulation of Turnaround Time and Manpower of Military RLVs," AIAA Paper 2004-6111, Sept. 2004.

[10] Hank, J. M., Franke, M. E., and Eklund, D. R., "TSTO Reusable Launch Vehicles Using Airbreathing Propulsion," AIAA Paper 2006-4962, July 2006.

[11] Orloff, B., "Comparative Analysis of Single Stage to Orbit Rocket and Air-Breathing Vehicles," M.S. Thesis, Air Force Institute of Technology, Wright–Patterson AFB, OH, June 2006.

J. Martin
Associate Editor